

# **Computational Modeling of Liquid Crystals and Related Materials**

## **Using Time-Dependent Density Functional Theory**

**Vinay Pendri**

Pittsford Mendon High School

Pittsford, New York

Advisor: Kenneth L. Marshall

**Laboratory for Laser Energetics**

University of Rochester

Rochester, NY

September 2023

## **Abstract**

The change in electron density distribution of saturated and unsaturated liquid crystals (LC's) and related molecules in response to 113-fs gaussian laser pulses was modeled computationally using real-time time-dependent density functional theory (rt-TDDFT) with the molecular modeling software *NW Chem*. Calculations were conducted using three different orientations of 900 nm linear polarized light incident on two molecules, one saturated and one unsaturated, to study the change in electron density as a function of incident laser polarization. Results show a significant difference between the localized electron densities of CB15 and CCH, the two molecules of interest, resulting from their differences in saturation. This work will serve as the basis for further investigation of rt-TDDFT's applications in LC and optics research to model areas of application interest such as photochemical reactions, laser damage resistance, polarizability and dielectric constant.

## 1. Introduction

Liquid crystals (LC's) are a form of matter in between a crystalline solid and an isotropic liquid. The highly organized structure of LC's creates optical effects in short path lengths much more effectively than conventional optical materials. As a result, LC's are employed in high-energy laser systems in circular polarizers and waveplates [1].

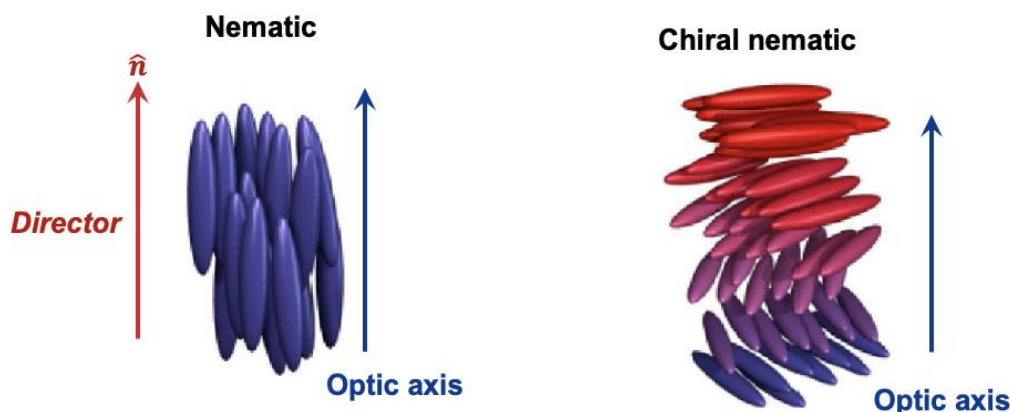


**Figure 1:** Nematic and chiral nematic phases of LCs. The optic axis in nematic LC's is parallel to the long molecular optic axis, whereas once a dopant is added to a nematic LC, the chiral nematic LC mixture has an optic axis that is normal to the long molecular axes. The helical structure of chiral nematic LC's is induced by the chiral (asymmetric) functional groups of dopants. [1]

The three main phases of LCs are nematic, cholesteric, and smectic. This work considers the nematic phase of LC's. Primary applications of nematic LC's are in liquid crystal display (LCD) technology, but they are also frequently used in mixtures with chiral "dopant" materials. The dopants may or may not be LC's. These dopants impart their chirality (twist sense) to the nematic LCs as seen in Fig. 1. Chirality is defined as the intrinsic handedness of a molecule, meaning it is not superimposable onto its mirror

image [2]. Chiral dopants are of interest in optical applications as well because they allow chiral nematic LC mixtures to selectively reflect light by changing the chirality of the host nematic LC mixture [3].

In high-energy laser systems, light passing through the chiral nematic LC mixtures can induce damage by potentially affecting their localized electron density. Electron density is the general representation of the probability of finding an electron in a certain area of an atom or molecule. This factor is important in modeling laser damage in LC's because electron density affects both the chemistry and the optical properties of an LC mixture [2]. The degree of saturation of the LC molecule has a substantial effect on the degree of electron density changes, which in turn impact other optical properties such as dielectric anisotropy and polarizability – respectively, the differences in dielectric responses in different directions and the tendency to induce dipole moments [3].

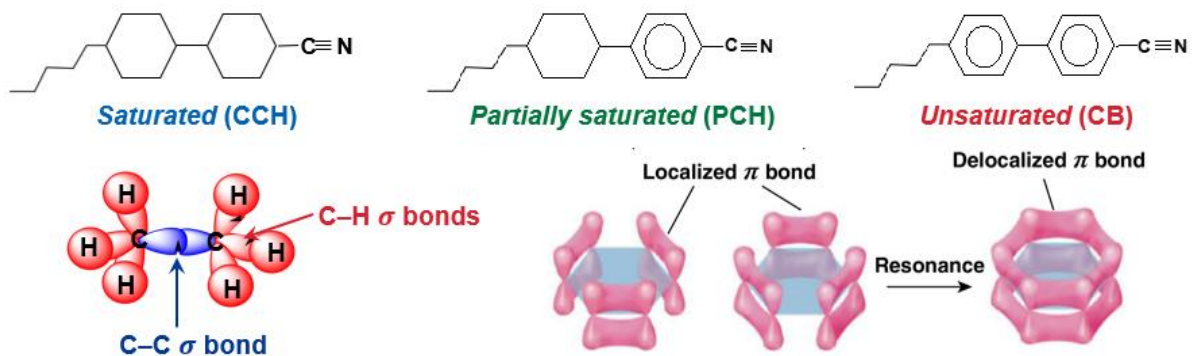


**Figure 2:** CCH, PCH, and 5CB (similar to CB15) molecular structures. Delocalized  $\pi$  bonds in the unsaturated 5CB molecule loosely hold electrons while  $\sigma$  bonds in the saturated CCH molecule tightly hold electrons. [1]

The two molecules used to investigate this phenomenon were 4'-(2-methylbutyl)-4-cyanobiphenyl (CB15) and 4'-pentyl-[1,1'-bi(cyclohexane)]-4-carbonitrile (CCH). Figure 2 shows that there are also variations of these molecules, such as 4-(4-

pentylcyclohexyl)benzotrile (PCH), that have one saturated and one unsaturated ring. CB15 is an unsaturated molecule with  $sp$  hybridization in the ring structures of the molecule, meaning that it has loosely held electrons in delocalized  $\pi$  bonds. In contrast, CCH is a fully saturated molecule with  $sp^3$  hybridization in the ring; it is composed of fully saturated hydrocarbons with only carbon-carbon single bonds [4]. As seen in Fig. 2, the saturated CCH molecule has sigma bonds with tightly held electrons and no  $p$ -orbitals available for delocalization. All three of these examples, CB15, PCH, and CCH, are of interest for use in high-energy laser optics.

CB15, which is chiral but not an LC, is used as the dopant in chiral nematic LC mixtures used on the OMEGA laser at the Laboratory for Laser Energetics. CCH is a non-chiral LC, but with a minor substitution on the hydrocarbon chain on the left of Fig. 2 could be made chiral. Such a modified CCH is of great interest as a potential replacement with a higher damage threshold for the dopant CB15. Since the damage susceptibility and other properties of CCH and modified CCH molecules depend primarily on the ring structures, the results obtained here for CCH are expected to be valid for the modified molecules.

In order to model how CB15's and CCH's electron densities are affected by high-energy laser pulses and what role the degree of saturation plays in this process, this study used real-time time-dependent density functional theory (rt-TDDFT) [3]. Computational modeling is a much more efficient and cost-effective method for learning about LC properties than manually synthesizing and testing compounds in the laboratory. The main advantage of computational modeling is that a large variety of LC compounds can be

screened simultaneously based on structures and properties, which helps to identify only those compounds that would have the highest probability of possessing the desired properties. This approach minimizes (but doesn't eliminate) the need to synthesize highly complex compounds for testing (which can be difficult for highly chiral structures) and allows one to gain important understandings of molecular interactions that would otherwise be difficult to attain in the lab. An additional benefit is the ability to achieve a deeper understanding of the quantum mechanisms behind the various useful properties of LC's and even predict the chemical and optical properties of yet-to-be synthesized LC's, such as the modified CCH molecules.

## **2. Previous Research**

There are three main methods to perform excited state calculations for a given molecule: *ab initio*, semi empirical, and density functional theory (DFT) [3].

*Ab initio*, meaning "from the beginning," is an "umbrella" term covering different computational methods such as Hartree-Fock and Configuration Interaction Singles (CIS) [3]. Although *ab initio* can provide higher accuracy excited state calculations than other known methods, it is extremely computationally intensive due to the need to conduct electron orbital calculations and scale up for larger molecules. For instance, the Hartree-Fock method uses the idea that every electron's path is characterized by a single particle function or orbital that doesn't depend on the motion of other particles in the system. The CIS method is similar to Hartree-Fock and incorporates varying electron shells and excitations, but it can only calculate single excitations. Both techniques require starting from basic principles to calculate excited states and heavily neglect electron-

electron interactions and relativistic effects [2]. The result is high computational demand with decreasing accuracy as the size and complexity of the molecules increases, where it is impossible to ignore the interactions of electrons.

In contrast to *ab initio*, the semi-empirical method uses experimental data to fit parameters to reduce computational time. The most common type of semiempirical excited state calculation is Zerner's Intermediate Neglect of Differential Overlap (ZINDO). This method uses superpositions of wavefunctions constructed from ground state orbital configurations [2] and ignores interactions between orbitals, but can account for spin-orbit interactions, which is useful for studying molecular systems with heavier, complex atoms. The use of estimates based on prior data allows for greatly reduced computational time, but less accurate results when compared to other methods such as DFT [2].

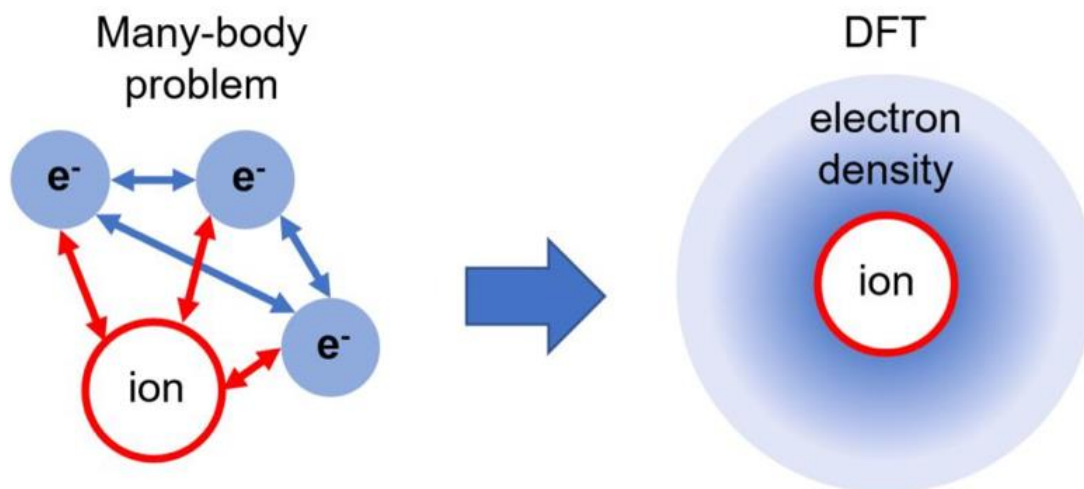


**Figure 3:** The many-body problem in regular excited state calculations and electron density used in DFT. The use of electron density eliminates the computational complexity of the many-body problem [6].

DFT falls between *ab initio* and semi-empirical methods in terms of accuracy and computational intensity. As seen in Fig. 3, DFT replaces the complex many-electron wavefunctions with a three-dimensional spatial function that provides electron density. Since DFT uses electron density in its calculations, it does not rely on the many-electron wavefunction, which contributes to much of the computational strain in the *ab initio* and semi-empirical methods. In the time-dependent Schrödinger equation as seen in Fig. 4, the Hamiltonian energy operator  $\hat{H}(t)$  accounts for the energy in the system. Plugging the Hamiltonian operator into the Schrödinger equation solves for the wave function, which gives the system's properties, including electron density [3].

$\hat{H}(t)\Psi(t) = i\frac{\partial\Psi(t)}{\partial t}$	$\hat{H}(t) = \hat{T} + \hat{V}_{ee} + \hat{V}_{\text{ext}}(t)$
<b><u>Time-dependent Schrödinger Equation</u></b>	<b><u>Hamiltonian energy operator</u></b>
<p><math>\hat{H}(t)</math> = Hamiltonian energy operator  <math>\Psi(t)</math> = wavefunction</p>	<p><math>\hat{H}(t)</math> = Hamiltonian energy operator  <math>\hat{T}</math> = kinetic energy  <math>\hat{V}_{ee}</math> = electron electron repulsion  <math>\hat{V}_{\text{ext}}</math> = external potential (laser pulse)</p>

**Figure 4:** The Time-dependent Schrodinger Equation and Hamiltonian energy operator.

This idea of using the Time-dependent Schrodinger Equation and Hamiltonian energy operator to input external factors is applied to TDDFT to model disturbances, such as electric fields and laser pulses, that interact with the electron density of a molecule. The variation of TDDFT used in this experiment is rt-TDDFT, which incorporates an external electric field and captures real-time electron density evolution [5]. These time-

dependent calculations can also provide a way to find absorption and emission spectra as well as dielectric constant and polarizability [2].

### 3. Methodology

The excited state calculations were carried out on the CB15 and CCH molecules after they were first constructed and geometry optimized using the *Maestro* graphical user interface and *Jaguar* computational module in the *Schrödinger Material Science Suite* (see Fig. 5). The atoms, bonds, and bond angles were constructed using *Maestro*'s building tools [7]. Then *Jaguar* checked inputted information to ensure it could undergo the energy minimization [8]. This process covered one hundred iterations and optimized the molecule's geometry to minimize energy.

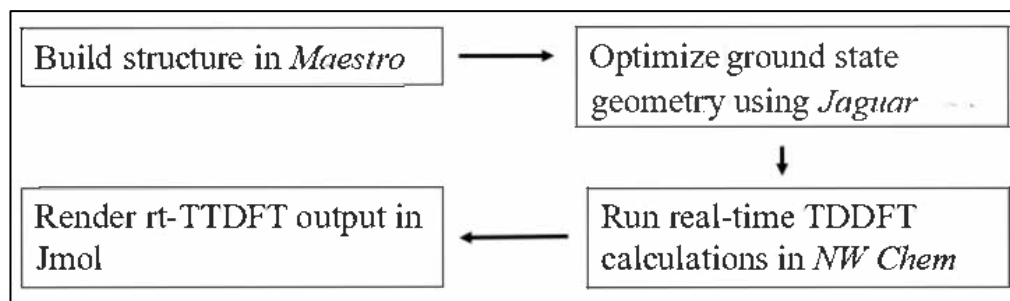


**Figure 5:** Methodology overview.

As depicted in Fig. 6, the next step was to input the energy-minimized molecular structures from *Maestro* into *NW Chem*, where rt-TDDFT calculations were performed [5]. The default basis set, 6-311++G, and hybrid functional, B3LYP, were used for preliminary DFT calculations. A basis set is a collection of functions that represent the electron wave functions of a molecule [3]. The selected sets are usually localized around each atom and impact the accuracy of the DFT calculation. The hybrid functional merges

the exchange correlation energy functional and Hartree Fock density functional in order to adjust for the underestimation of bond strength in DFT. Hybrid functionals also improve the accuracy of excited state calculations [2].

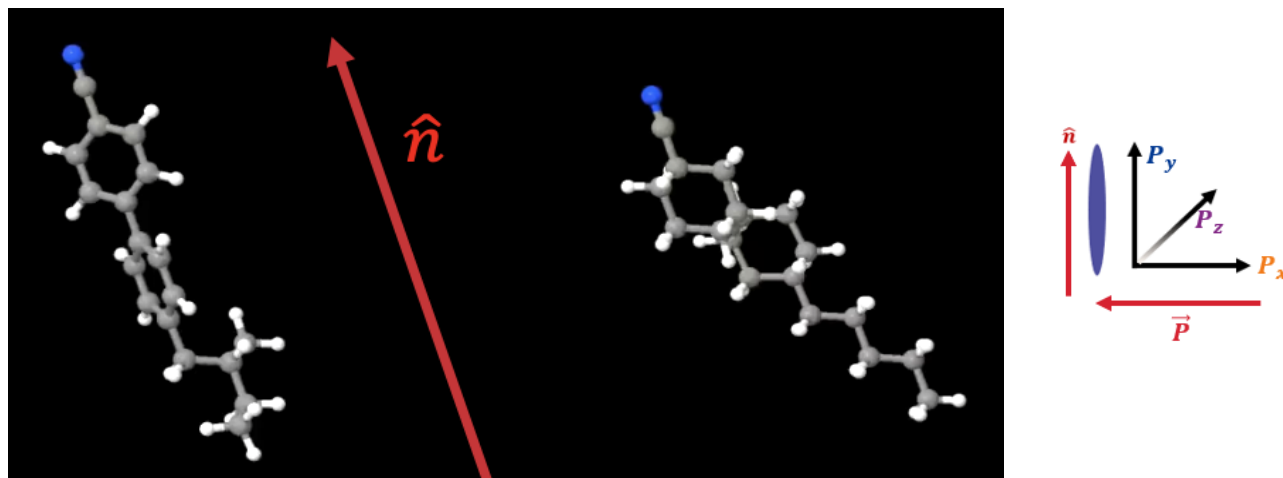


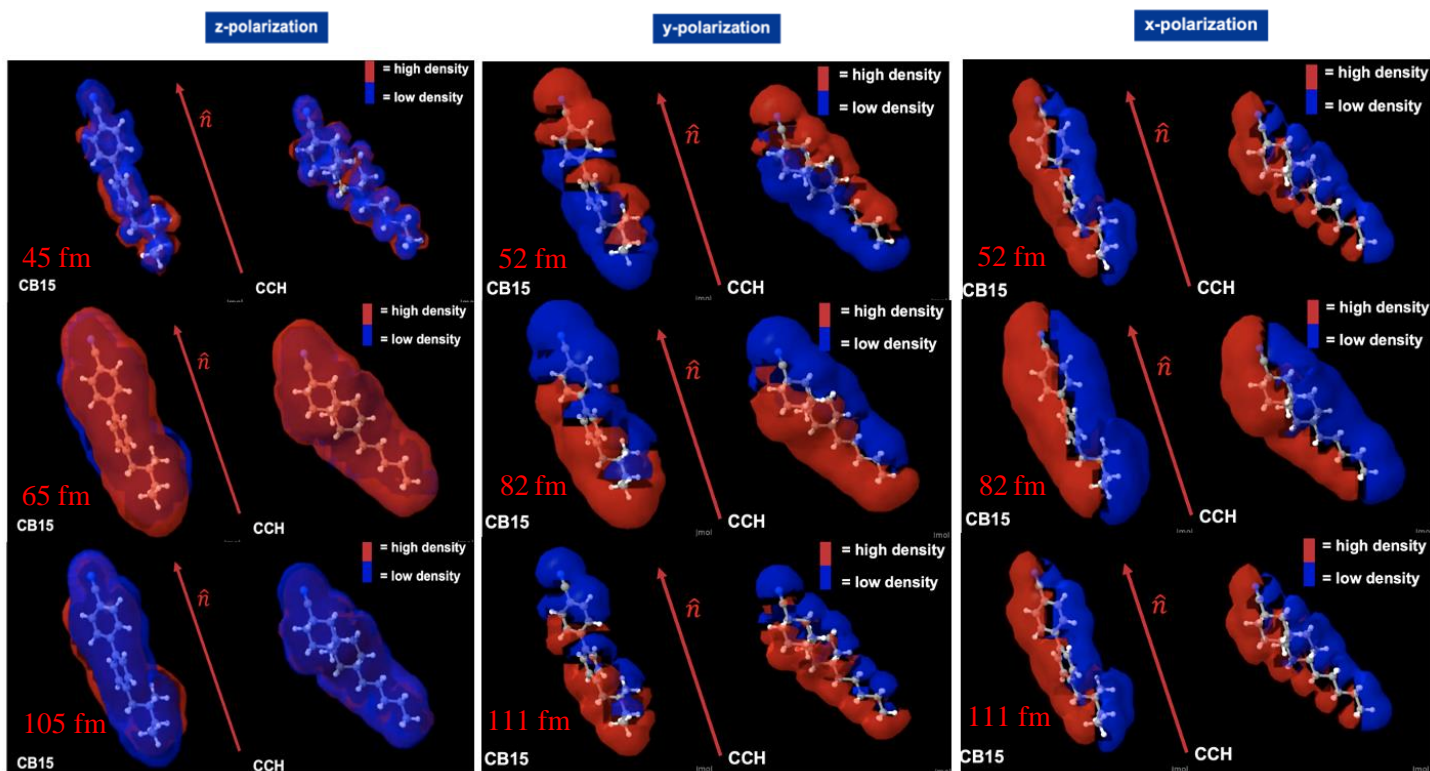
**Figure 6:** Optimized energy structures inputted into NW Chem. CB15 (left) and CCH (right) are shown with respect to the director  $\hat{n}$ . The director is the net average direction of the long molecular axis of the molecules in the condensed phase [4]. X, y, and z light polarization directions ( $P_x$ ,  $P_y$ ,  $P_z$ ) are displayed in the graphic (right).

The rt-TDDFT calculations simulated a 900-nm 113-fs Gaussian laser pulse that was polarized with respect to the x, y, and z axes in three separate trials as seen in the small graphic on the right side of Fig. 6. The 900 nm wavelength was chosen to minimize the impact of optical absorbance and selective reflection that can occur at the 351 and 1053 nm wavelengths. To maximize use of computational resources, this study modeled 65% of the 113-fs Gaussian laser pulse width applied in each simulation. Single molecules in the gas phase were used to minimize the complexity of calculations that would be introduced by electrostatic and Van der Waals forces of neighboring molecules in the condensed phase. The 113-fs time frame was chosen as a compromise to both minimize computational load but still capture the electron density at peak intensity and directly after

the peak. Conducting these same calculations over a broader temporal range (ps) was estimated to take up to *40 years* using six nodes and 240 cores on the LLE supercomputing cluster DELUGE with a total of six simulations run for each polarization of light on each molecule. Total computational times for the femtosecond laser pulse regime were around 168 hours for each incident polarization modeled. Calculations for each polarization direction for CB-15 took 54 hours, while similar calculations on CCH took ~75 hours. This increased computational time can be attributed to a larger number of electron-electron interactions in the saturated CCH molecule.

#### **4. Results and Discussions**

Excited state electron densities were calculated for CB15 and CCH for x, y, and z polarized Gaussian laser pulses. The results are show in Fig. 7, rendered using Jmol [9]. Significant differences in the electron densities of CB15 and CCH among different polarizations of light and between the molecules can be seen.



$\vec{P}$  = propagation direction  
 $\hat{n}$  = director  
 $P_n$  = Polarized in the  $n$  direction

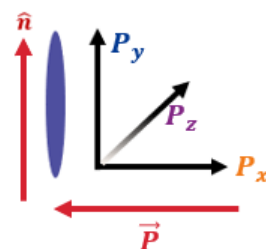


**Figure 7:** Time-resolved snapshots of rt-TDDFT electron density maps for CB-15 and CCH for each incident polarization of light. The portion of the femtosecond pulse width represented by each set of electron density maps is shown beneath each map. The vector diagram defines the coordinate axes, the director orientation, and, for z and y polarizations, laser pulse propagation direction. For x polarization, the propagation is along the y direction.

The incident polarization angle of the laser affects the electron-rich and electron-poor hemispheres of the molecules and suggests that light polarization may vary the impact on electron density. The polarization of the electric field is seen to oscillate perpendicular to the propagation axis. In the simulation, the laser pulse polarization also describes the direction of the electric field's oscillations. Figure 7 shows that the high electron density and low electron density area fluctuations are a response to the varying external electric field polarizations.

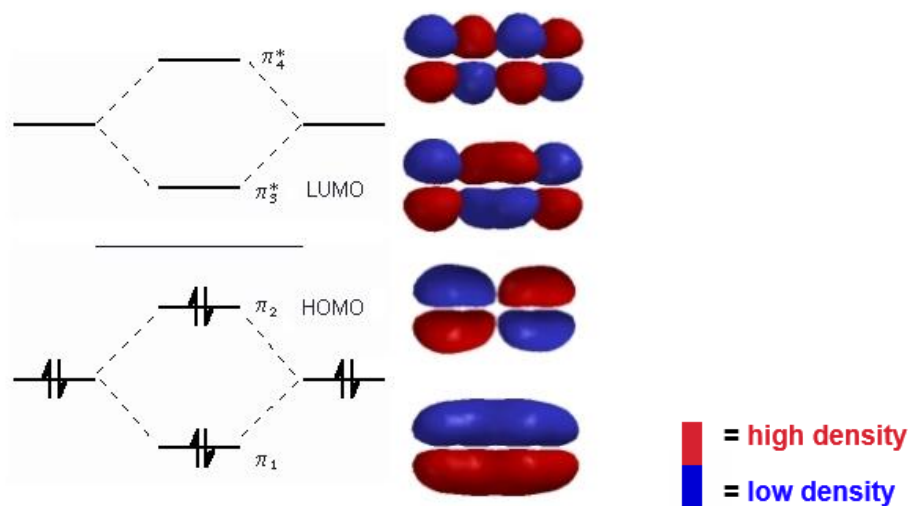


**Figure 8:** Example of HOMO LUMO transitions in molecules. The delocalized  $\pi$  electrons cause the electron densities to vary [4]. The variously numbered  $\pi$  symbols represent the energy states of each electron.

Figure 7 shows that there is a significant difference between the localized electron densities of CB15 and CCH. This is due to differences in saturation. Displayed in Fig. 8, this phenomenon is due to the delocalized  $\pi$  bonds and electrons present in CB15 that contribute to HOMO (Highest Occupied Molecular Orbital) and LUMO (Lowest Unoccupied Molecular Orbital) energy transitions [3]. When a delocalized  $\pi$  electron in an unsaturated molecule like CB15 is excited, changes in the electronic energy of the

molecule occur. The cloud-like formation of  $\pi$  electrons can allow for larger changes in the molecule when perturbed. Figure 7 displays that the electron densities shift to the director's direction of both molecules during the simulation, but more so in CB15 due to greater numbers of  $\pi$  electrons.

## 5. Conclusions

Real-time TDDFT was used to calculate the excited state electron densities of the molecules CB15 and CCH when perturbed by 900 nm, 113 fs Gaussian test pulses of x, y, and z, polarizations. A methodology has been developed to perform rt-TDDFT calculations on molecules and render images through Jmol in order to capture electron density. The temporal variations of electron density depend on the molecules' inherent  $\pi$ -electron delocalization, the propagation direction, and the incident laser polarization angle relative to the long molecular axis.

This study is the first step into the computational modeling of dopants used in chiral nematic LC mixtures employed in high energy optics, and gives insights on the changes in electron density distribution probabilities during the initial and peak portions of the incident femtosecond-regime pulse. Of even more significance is what happens to the electron density distribution on the trailing portion of the pulse, as non-reversible changes in electron density could indicate the onset of chemical reactions that could be precursors to laser-induced damage (Fig 9).

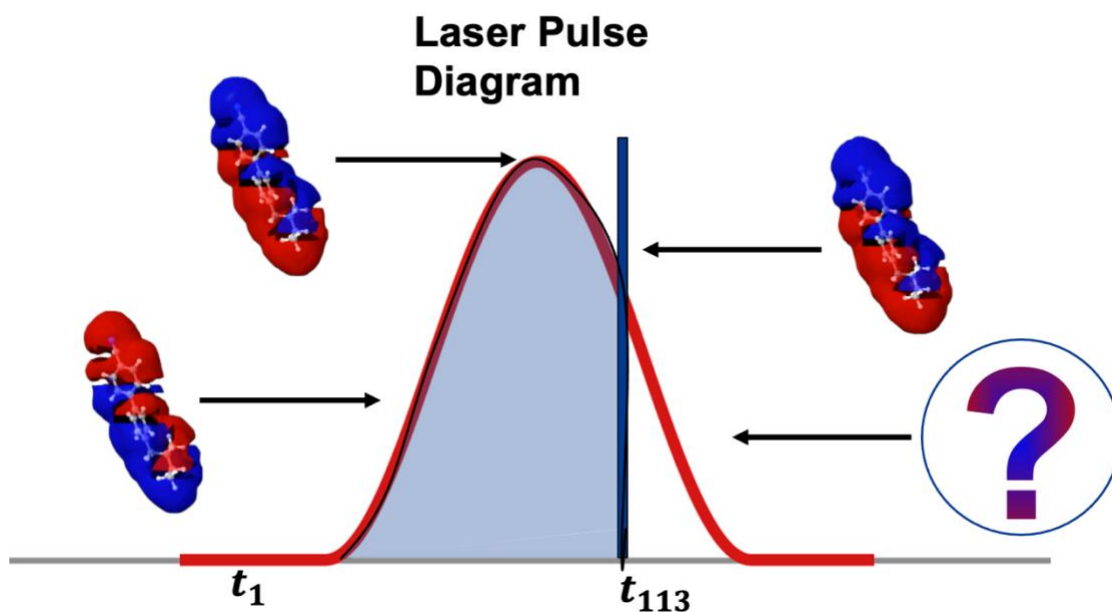


**Figure 9:** Laser pulse diagram showing the need for future work modeling the pulse decline, since the pulse's incline and peak have already been modeled. The images shown are taken from Fig. 7 for CB15 and y polarization.

The success of this method will aid the future development of computational models using electron density to efficiently determine the properties of novel LC materials and better understand the complex mechanisms behind the many useful qualities of these materials. This information is also useful for determining potential decomposition methods for molecules such as CB15 and CCH. This study determined that there is a difference in electron density reactions between different light polarizations, but this phenomenon requires further research in order to better understand the reasons behind it. The saturation levels of CB15 and CCH also affect the electron densities by varying the rate at which the electron density changes.

In this study, the default basis set and hybrid functional were used, so further investigation into different basis sets and hybrid functionals is needed to determine the optimal combination. Once basis sets are optimized, future work can commence on molecular dynamics to involve the solvent in simulations, since current simulations only focus on the electron densities of dopant molecules. This is important because the solvent is just as essential to LC solutions as the dopant.

## **6. Acknowledgments**

I thank Dr. Stephen Craxton for the incredible opportunity to conduct research at LLE; Mr. Kenneth L. Marshall for his endless support and guidance throughout the research process; Dr. Nathaniel Urban for his advice and technical guidance; Dr. William Scullin and Dr. Kenneth Anderson for their assistance in accessing and using computational resources; Julia Kubes and Leonid Solodov for their mentorship; Ms. Kim Truebger for managing the program's logistics; Jacob Deats and Eugene Kowaluk for their photography. Lastly, I am grateful to the University of Rochester, the U.S. Department of Energy, and the National Nuclear Security Administration for funding this research.

## References

- [1] Marshall, K. L. et al; "The Effect of Incident Polarization Handedness and Ellipticity on the Laser-Damage Resistance of Oriented Liquid Crystals in the Nanosecond Regime" (Conference Presentation); SPIE proceedings, October 2021.
- [2] Wang, R., "Computational Modeling of Spectral Properties of Nickel Dithiolenes"; LLE Summer High School Research Program, 2006.
- [3] Collings, P. J. and Patel, J. S., Handbook of Liquid Crystal Research, Oxford University Press, 1997.
- [4] Vollhardt, K. Peter C. and Schore, Neil E. Organic Chemistry: Structure and Function. Fifth Edition. New York, N.Y.: W. H. Freeman Company, 2007.
- [5] Real-Time TDDFT, NWChem, <https://nwchemgit.github.io/RT-TDDFT.html>.
- [6] Posysaev, S., "Applications of density functional theory for modeling metal-semiconductor contacts, reaction pathways, and calculating oxidation states," University of Oulu Graduate School Report Series in Physical Sciences, Report No. 123, 2018.
- [7] Schrödinger Release 2023-2: Maestro, Schrödinger, LLC, New York, info@schrodinger.com, 2023.
- [8] Bochevarov, A.D.; Harder, E.; Hughes, T.F.; Greenwood, J.R.; Braden, D.A.; Philipp, D.M.; Rinaldo, D.; Halls, M.D.; Zhang, J.; Friesner, R.A., "Jaguar: A high-performance quantum chemistry software program with strengths in life and materials sciences," Int. J. Quantum Chem., 113(18), 2110-2142, 2013.

[9] Jmol development team. (2016). Jmol. Retrieved from <http://jmol.sourceforge.net>.